Contemporary Mathematics
https://ojs.wiserpub.com/index.php/CM/

Research Article

Mean First-Passage Time in a Sphere Traversed by a Cylinder

Hélia Serrano[1*], Ramón F. Álvarez-Estrada[2]

[1] Department of Mathematics, Faculty of Chemical Sciences and Technologies, University of Castilla-La Mancha, Spain
[2] Department of Theoretical Physics, Faculty of Physics, Complutense University of Madrid, Spain
E-mail: heliac.pereira@uclm.es

Received: 31 July 2025; **Revised:** 13 September 2025; **Accepted:** 22 September 2025

Abstract: We study Mean First-Passage Times (MFPTs) for diffusive migration in finite three-dimensional domains motivated by organ-vessel architectures and intracellular transport. Focusing on a sphere traversed by a thin cylinder (an idealised organ surrounding a blood vessel), and on a deformed hollow sphere with an inner trap, we formulate MFPT via boundary integral equations that encode Dirichlet, Neumann, and Robin conditions. Two complementary strategies emerge: (i) a deformation-from-solvable-geometry approach that yields accurate approximations for mixed boundaries, and (ii) a "conductor-term" augmentation that restores solvability when standard integral equations fail. These frameworks expose narrow escape/capture regimes and quantify how trap size and interface semi-permeability control MFPT. We complement theory with numerical solutions of the adjoint Poisson problem, covering cases not reached analytically: first, a sphere with Dirichlet boundary condition, traversed by a cylinder with Neumann one (complementing the integral equations approach); second, a sphere with Neumann boundary condition, traversed by a cylinder with Dirichlet one (uncovered by the integral equations approach). Beyond methodological value, our results provide interpretable MFPT maps relevant to cell migration and particle delivery in organ-like geometries.

Keywords: mean first-passage time, Brownian motion, Poisson equation, Dirichlet, Neumann and Robin boundary conditions, sphere traversed by cylinder, narrow capture problem

MSC: 35K20, 45A05, 92C17

1. Introduction

Diffusive particle migration is a very important statistical transport phenomenon that arises and has different applications in biology, biochemistry, physics, and engineering. Here, we shall deal with diffusion without advection. One important approach to particle diffusion employs Green's functions, which depend generically on two position vectors and, eventually, on another variable related to time. To handle Green's functions with boundary conditions may be cumbersome. On the other hand, and, at least as long as time durations in particle migration and the understanding of boundary conditions are concerned, it is more economical to handle a simpler function of one position vector, namely, the so-called Mean First-Passage Time (MFPT) function. Calculating or estimating the MFPT is essential in several specific fields, from modelling chemical reactions to designing efficient nanoparticle-based drug delivery systems (see [1–16]).

DOI: https://doi.org/10.37256/cm.6620258087

The MFPT is the expected time for a Brownian particle, starting from an initial position within a confined domain, to reach for the first time a specified target location (in particular, the boundary of the domain). Once the imposition of boundary conditions be understood for the MFPT function, the extension to Green's functions appears to be conceptually rather direct, even if formulae are still rather cumbersome. Moreover, Green's functions have short-distance singularities, the control of which requires detailed analysis upon carrying out approximations. On the other hand, the MFPT functions either display such short-distance singularities in a simple way or do not have them. In fact, the MFPT functions are obtained by performing spatial integrations of Green's functions. In so doing, short-distance singularities of Green's functions are smoothed out.

In this work, we shall treat mostly the MFPT for a Brownian particle inside a sphere traversed by a thin cylinder, modelled by the Poisson equation with suitable mixed boundary conditions. Such a geometry is biologically motivated, as it resembles qualitatively a vital organ surrounding a blood vessel. Motivated by this analogy, we shall analyse different features of the associated MFPT to a large extent theoretically because, being non-trivial, they do deserve adequate analysis (but not exclusively: see Section 5 for numerical studies). In fact, that geometry, with different boundary conditions, does not yield a closed-form MFPT and, so, poses certain mathematical difficulties (as shown in Sections 2 and 4). In so doing, we come close to and treat a related mathematical difficulty, for another geometry (namely, a deformed hollow sphere with a trap inside), in Section 3.

The approach to the MFPT in the present work will extend non-trivially certain aspects in [17–20], not treated previously, which do deserve further and deeper analysis; namely, other adequately motivated geometries, Robin boundary conditions, and certain narrow escape cases. We shall remind the so-called potential theory [17], namely, a time-honoured mathematical theory for Electrostatics, formulated to deal with problems with Dirichlet and Neumann boundary conditions. In this theory, a function of interest (say, the electrostatic potential) inside a domain is represented as the sum of an explicit inhomogeneous term plus an integral over the boundary, containing a suitable Green's function and certain density functions. The latter satisfies, in turn, suitable inhomogeneous linear integral equations on the boundary, encoding the Dirichlet or Neumann boundary conditions non-trivially, with other inhomogeneous terms determined by the above explicit inhomogeneous term. The structure of those linear integral equations is deeply connected to the specific boundary conditions. The MFPT encodes how a migrating particle (or cell) interacts with interfaces. Dirichlet (absorbing) boundary captures at first contact (e.g., an exit through the organ boundary or irreversible adhesion) and leads to zero MFPT on the target. The Neumann (reflective) boundary is an impermeable wall with zero normal flux, so that the walker cannot cross, and the MFPTs increase near it. Robin (partially absorbing/transmissible) boundary interpolates continuously between absorbing and reflecting behaviour and models semi-permeable membranes. We use this mapping explicitly in Section 2 (absorbing sphere traversed by a transmissible cylinder), Section 4 (transmissible sphere with absorbing cylinder).

Compact solutions of those integral equations for the density functions exist only in a few geometries: spherical surfaces, concentric spherical surfaces, cylinders, and some others, provided that the boundary conditions are adequate. So will denote the set of all such restricted cases with Compact (C) Solutions (So). For more general boundary surfaces S, one proceeds through the following strategies.

First Strategy. Let a particle diffusion problem be determined by some surface S and boundary conditions not belonging to Compact Solutions (CSo), such that:

i) the boundary surface S either does not differ much from the surface S_{CSo} for one case belonging to CSo, or differs appreciably but in a mathematically controllable way.

ii) one chooses an explicit inhomogeneous term as a starting point, which may not be optimal.

iii) for the given particle diffusion problem, one represents initially its MFPT function and density functions in terms of that explicit inhomogeneous term plus integrals over the boundary S.

iv) the inhomogeneous linear integral equations resulting for density functions have kernels that allow the former to be well defined. Not infrequently, the fulfillment of iv) shows up at the first stages of the analysis.

v) one appeals to the compact MFPT solution and associated density functions for the surface S_{CSo} and, in terms of them, one recasts respectively the initial MFPT function and density functions for S into other forms as a second step, upon regarding S as a small or controllable deformation of S_{CSo}.

vi) the resulting equations do provide a suitable basis for the desired approximate MFPT solutions for S, through successive iterations.

The *First Strategy* will suffice for different cases of spheres traversed by thin cylinders (but it may not cover others), as we shall see.

To provide a wider perspective, we warn that, upon applying the *First Strategy* to the MFPT for certain boundary conditions, a difficulty may arise at item iv): the inhomogeneous linear integral equations for the density functions, as directly formulated, have no solutions. This is the direct extension to the integral equation framework of the well-known non-existence of an MFPT solution inside an undeformed spherical surface with Neumann boundary condition (in turn, bearing a relationship to the narrow escape problem). This motivates the following approach.

Second Strategy. The addition of suitable "conductor" surface terms leads to other inhomogeneous linear integral equations for the density functions at the level of step iv) which do have solutions, as we shall illustrate. Then, the steps v) and vi) of the *First Strategy* are carried out for the *Second Strategy*. This will be the case of a deformed hollow sphere with a trap inside.

In narrow capture situations, the MFPT stands specifically for the expected time required for the Brownian particle moving inside a bounded domain, typically with a reflective boundary, to escape the domain through a small absorbing region on the boundary, usually called the trap. The boundary surfaces, with possible disparate geometries and boundary conditions to be satisfied by the diffusive motions, give rise to non-trivial boundary value problems, which have attracted much attention. See [2, 3, 21–28] and references therein. These problems involve (at least, or typically) two spatial scales: the spatial scale of the confined domain, and the asymptotically small scale of the absorbing trap. A good number of research papers about them employed Green's functions: see, for instance, [21, 23] and references therein. The present integral equations approach and the above strategies enable us to analyse narrow capture situations and signals thereof, from another standpoint, as we shall see.

This work is organized as follows. In Section 2, the Brownian particle, moving inside an absorbing sphere traversed by a thin transmissible cylinder, is modelled by the Poisson equation with mixed Dirichlet (sphere) and Robin (cylinder) boundary conditions. No narrow capture situations arise for it. This is analysed with the *First Strategy.* In Section 3, we treat a reflective (Neumann) deformed hollow sphere with an inner absorbing (Dirichlet) spherical trap, where the narrow capture situation occurs: its analysis illustrates the *Second Strategy* in a simpler, but not trivial, context. In Section 4, a transmissible (Robin) sphere traversed by a thin absorbing (Dirichlet) cylindrical trap is considered with boundary conditions different from those in Section 2, in which the *First Strategy* suffices; however, a certain narrow capture situation is seen to arise, which is compared to that in Section 3. Section 5 presents numerical computations of the adjoint equation for the MFPT, for both geometries in Sections 2 and 4, for Dirichlet and Neumann boundary conditions. We emphasize that the numerical approach enables dealing with cases not covered by the integral equation approach. Finally, Section 6 outlines the conclusions and some discussions. Appendix A summarizes useful results in the integral equation approach to the MFPT and its density functions for a diffusing particle inside an absorbing spherical surface, for subsequent use in its counterpart with Robin boundary condition. Appendix B gives useful properties of Green's functions, in connection with Section 4.

2. Absorbing sphere traversed by a thin transmissible cylinder

In this section, the three-dimensional finite domain Ω is a sphere of radius R, with a very thin circular cylinder trap inside of it, with radius r, so that $R \gg r$, as in Figure 1. The centre of the sphere is chosen as the origin of coordinates, and the third z-axis is the symmetry axis of the cylinder. Let h_1 be the length $h_1 = \sqrt{R^2 - r^2}$ so that $R = h + h_1$. The intersections of the spherical surface S_{sph} and the cylindrical one are two circumferences, denoted by c_- and c_+, of radius r, lying in two parallel planes at $z = -h_1$ and $z = h_1$, respectively. Let S_c be the open cylindrical surface, parallel to its symmetry z-axis and determined by $-h_1 \leq z \leq h_1$, at a distance r from the z-axis. Let S_s be the open spherical surface of radius R, limited by the two circumferences discussed above, inside S_{sph}. Therefore, Ω is bounded by the outer open spherical surface S_s and the inner cylindrical one S_c and, so, doubly-connected. The closed surface S enclosing Ω is given by $S = S_s \cup S_c$.

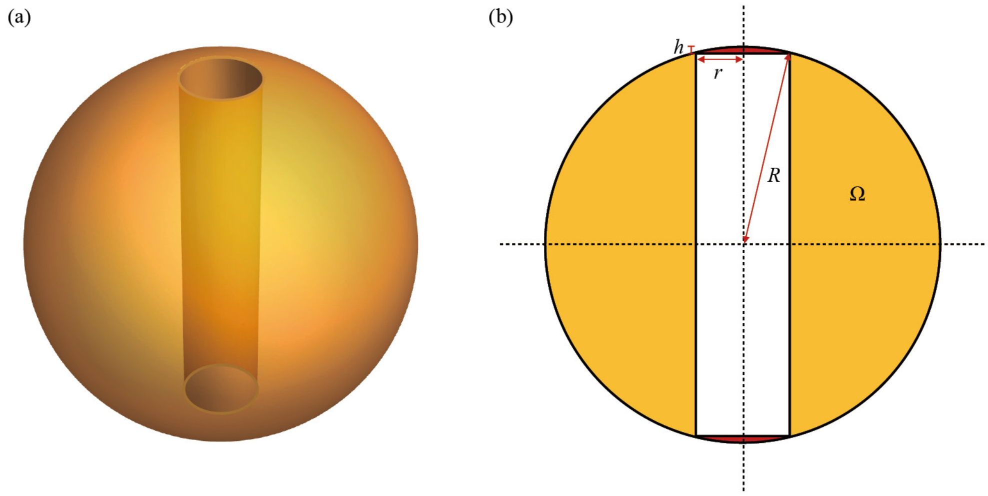

Figure 1. In the panel (a), the domain Ω enclosed by the spherical surface of radius R traversed by the circular cylinder of radius r. In the panel (b), its projection into the ZY-plane

Let us formulate the boundary conditions of our domain Ω. Let the particle, moving inside the domain, reach the outer spherical surface S_s and leave Ω. In this way, the MFPT function satisfies an absorbing (Dirichlet) boundary condition on S_s. On the other hand, we assume that the inner cylindrical surface S_c is transmissible (Robin boundary condition). Thus, we are interested in studying the MFPT function T that satisfies the Poisson equation with mixed Dirichlet-Robin boundary conditions of type

$$D\Delta T(x) = -1 \text{ in } \Omega, \tag{1}$$

$$\lim_{x \to y} T(x) = 0 \text{ on } S_s, \tag{2}$$

$$a \lim_{x \to y} \frac{\partial T}{\partial n}(x) + b \lim_{x \to y} T(x) + c = 0 \text{ on } S_c, \tag{3}$$

$a \neq 0$ (representing absorption)), b (representing reflection), and c (contributing to implement that absorption and reflection are not complete) are real constants. Δ is the standard Laplacian. The limits are always taken from inside Ω. $\frac{\partial T}{\partial n}$ denotes always the inner normal derivative, from inside Ω. D is the diffusion coefficient. Due to the above choice of boundary conditions, this model will illustrate the *First Strategy* nontrivially. The present case and the one in Section 4 correspond to mixed boundary conditions, in the sense that in each of them the boundary conditions are not the same on different parts of the same surface S, namely, on S_s and S_c.

2.1 *Inhomogeneous linear integral equations for density functions*

Let $T_\infty(x) = -\frac{|x|^2}{6D}$ denote the solution of the Poisson equation (1) in infinite volume. Also, let L_∞ be the Green's function solving the diffusion equation

$$(D\Delta_x - s)L_\infty(x, y, s) = -\delta(x-y)$$

in infinite volume, where δ stands for the three-dimensional Dirac delta function. We shall only employ its restriction for $s = 0$ given by $L_\infty(x, y, 0) = \dfrac{1}{4\pi D}\dfrac{1}{|x-y|}$. Thus, the MFPT function T solution of the Poisson equation (1), subject to boundary conditions (2) and (3) in Ω, is defined by

$$T(x) = T_\infty(x) + \int_{S_s} \frac{\partial L_\infty(x, y, 0)}{\partial n(y)} \mu_s(y)\, dS(y) + \int_{S_c} L_\infty(x, y, 0)\mu_c(y)\, dS(y), \tag{4}$$

where the densities μ_s and μ_c are given in S_s and S_c, respectively, as the solution of the inhomogeneous system of linear integral equations

$$\mu_s(y) = -2DT_\infty(y) - 2D\int_{S_s} \frac{\partial L_\infty(y, z, 0)}{\partial n(z)} \mu_s(z)\, dS(z) - 2D\int_{S_c} L_\infty(y, z, 0)\mu_c(z)\, dS(z), \tag{5}$$

$$\mu_c(y) = \frac{1}{a}\left(a\frac{\partial}{\partial n(y)} + b\right)\left(2DT_\infty(y) + 2D\int_{S_s} \frac{\partial L_\infty(y, z, 0)}{\partial n(z)} \mu_s(z)\, dS(z) + 2D\int_{S_c} L_\infty(y, z, 0)\mu_c(z)\, dS(z)\right) + \frac{2Dc}{a}. \tag{6}$$

The derivations for Dirichlet and Neumann boundary conditions in [18] can be directly generalized for Robin ones, so as to establish the validity of (6), details will be omitted.

Notice that T_∞, even if an allowed choice as an inhomogeneous term, is negative and, so, is not optimal, because an infinite number of successive iterations of the integral equations appear to be required to get a positive MFPT function. Anyway, the above three coupled inhomogeneous linear integral equations for T, μ_s, and μ_c are an adequate starting point: they are correct, hold without approximations, and do have solutions, as will be shown below.

2.2 *Implementing the First Strategy*

For the complete spherical surface S_{sph} with absorbing boundary condition, the MFPT T_{sph} is known exactly, as summarized in Appendix A. Then, such a case belongs to CSo. The purpose of the following transformations will be to express μ_s and μ_c for the present sphere plus cylinder case as the sum of dominant contributions (associated with S_{sph}), plus small contributions arising from small surfaces.

Notice that equation (5), as it stands, involves both on its left- and right-hand-sides, as it stands, values of μ_s only on S_s, which is part of S_{sph}. It turns out that L_∞ and its normal derivatives depend explicitly on vectors defined over the whole S_{sph}. That, still having values of μ_s for z only on S_s inside the relevant integral in the right-hand side of (5), allows us to extend the right-hand side of (5) to any y on S_{sph}. For justification of this extension in a different case, see [18]. Let S_h be the open "berets" of S_{sph} such that the union of S_s and S_h is precisely S_{sph}, ie $S_{\text{sph}} = S_s \cup S_h$. The open surface S_h is formed by two open surfaces limited by c_+ and c_-. This enables us to define μ_s for y on S_h and, then, over the whole S_{sph} in the left-hand sides of equations (7), (8), and (9). That extension of μ_s to S_h will be used below. It follows that

$$\mu_s(y) = -2DT_\infty(y) - 2D\int_{S_{\text{sph}}} \frac{\partial L_\infty(y, z, 0)}{\partial n(z)} \mu_s(z) dS(z)$$

$$+2D\int_{S_h} \frac{\partial L_\infty(y, z, 0)}{\partial n(z)} \mu_s(z) dS(z) - 2D\int_{S_c} L_\infty(y, z, 0)\mu_c(z) dS(z). \tag{7}$$

Notice that we have added and subtracted the term

$$2D\int_{S_h} \frac{\partial L_\infty(y, z, 0)}{\partial n(z)} \mu_s(z)\, dS(z).$$

It has enabled to write $-2D\int_{S_{\text{sph}}} \frac{\partial L_\infty(y, z, 0)}{\partial n(z)} \mu_s(z)\, dS(z)$ in (7) for y over the whole S_{sph} which, in turn, will allow to perform the inversion with the kernel $(I - K_{\text{sph}})^{-1}$, as indicated below. Such addition and subtraction and related ones, later on, will play a crucial role for the approximations. S_c and S_h are small surfaces (compared to S_{sph}).

By invoking Appendix A, we use the inverse kernel $(I - K_{\text{sph}})^{-1}$ defined in Appendix A. In so doing, we shall implement the *First Strategy*. Then, we rewrite μ_s in (7) as

$$\mu_s(y) = \int (I - K_{\text{sph}})^{-1}(\alpha(y), \alpha(z)) \Bigg[-2DT_\infty(z) + 2D\int_{S_h} \frac{\partial L_\infty(z, x, 0)}{\partial n(x)} \mu_s(x)\, dS(x)$$

$$-2D\int_{S_c} L_\infty(z, x, 0)\mu_c(x)\, dS(x) \Bigg] d\alpha(z), \tag{8}$$

α's denoting solid angles (see Appendix A). By recalling μ_{sph} in (60), μ_s in (8) reads

$$\mu_s(y) = \mu_{\text{sph}}(y) + \int (I - K_{\text{sph}})^{-1}(\alpha(y), \alpha(z)) \Bigg[2D\int_{S_h} \frac{\partial L_\infty(z, x, 0)}{\partial n(x)} \mu_s(x)\, dS(x)$$

$$-2D\int_{S_c} L_\infty(z, x, 0)\mu_c(x)\, dS(x) \Bigg] d\alpha(z). \tag{9}$$

By using the values of μ_s on the surface S_h, we rewrite μ_c in (6) as

$$\mu_c(y) = 2D\left(a\frac{\partial}{\partial n(z)} + b \right)\Bigg(T_\infty(y) + \int_{S_{\text{sph}}} \frac{\partial L_\infty(y, z, 0)}{\partial n(z)} \mu_{\text{sph}}(z)\, dS(z) + \int_{S_{\text{sph}}} \frac{\partial L_\infty(y, z, 0)}{\partial n(z)} (\mu_s(z)$$

$$-\mu_{\text{sph}}(z))\, dS(z) + \int_{S_c} L_\infty(y, z, 0)\mu_c(z)\, dS(z) - \int_{S_h} \frac{\partial L_\infty(y, z, 0)}{\partial n(z)} \mu_s(z)\, dS(z) \Bigg) + \frac{2Dc}{a}. \tag{10}$$

Let $T_{\text{sph}}(x) = \dfrac{R^2-|x|^2}{6D}$ be the MFPT function in a sphere of radius R with absorbing boundary condition, as given in (61). By using (55) for $T(x) = T_{\text{sph}}(x)$, we rewrite μ_c in (10) as

$$\mu_c(y) = 2D\left(a\frac{\partial}{\partial n(y)}+b\right)\left(T_{\text{sph}}(y)+\int_{S_{\text{sph}}}\frac{\partial L_\infty(y,\,z,\,0)}{\partial n(z)}(\mu_s(z)-\mu_{\text{sph}}(z))dS(z)+\right.$$

$$\left.+\int_{S_c}L_\infty(y,\,z,\,0)\mu_c(z)\,dS(z)-\int_{S_h}\frac{\partial L_\infty(y,\,z,\,0)}{\partial n(z)}\mu_s(z)\,dS(z)\right)+\frac{2Dc}{a}. \tag{11}$$

By proceeding like in (10) through (11), the MFPT in (4) reads

$$T(x) = T_{\text{sph}}(x)+\int_{S_{\text{sph}}}\frac{\partial L_\infty(x,\,y,\,0)}{\partial n(y)}\left(\mu_s(y)-\mu_{\text{sph}}(y)\right)dS(y)$$

$$+\int_{S_c}L_\infty(x,\,y,\,0)\mu_c(y)dS(y)-\int_{S_h}\frac{\partial L_\infty(x,\,y,\,0)}{\partial n(y)}\mu_s(y)dS(y), \tag{12}$$

where μ_s is defined on S_h as before. The characterization of the densities μ_s and μ_c, and the MFPT in (9), (11) and (12), respectively, involve no approximation. Contrary to $T_\infty(<0)$ in (4), $T_{\text{sph}}(>0)$ in (12) is adequate, as a consequence of the infinite number of iterations involved in $(I-K_{\text{sph}})^{-1}$. It is natural to accept that particle migration has cylindrical symmetry around the cylinder axis. Consequently, T, μ_s and μ_c will be independent on angles about the axis of the cylinder.

T_{sph} and μ_{sph} play here the role of the compact MFPT solution T_{CSo} and its associated density function, respectively, for the actual $S_{\text{CSo}} = S_{\text{sph}}$. Thus, T and its density functions μ_s and μ_c, upon regarding S as a controllable or small deformation of S_{CSo}, have been recast into the above new equations, which do provide a suitable basis for the approximate determination of the MFPT, through successive iterations.

2.3 *Low order corrections*

We shall solve equations (10) and (11) to get the MFPT function in (12) by successive approximations: we shall focus on the low-order ones. Thus, $S = S_s\cup S_c$, with S_c small, and S_s being a close approximation to the closed spherical surface S_{sph} of radius R. The small dimensionless parameter governing the approximation will be the ratio of the total area of the small surface $S_c\cup S_h$ over that of the larger S_s. We shall denote, in an obvious notation (identifying surface to its area), that small parameter as $(S_c\cup S_h)\setminus S_s$. For small $(S_c\cup S_h)\setminus S_s$, let $\mu_s \simeq \mu_{\text{sph}}+\mu_s^{(1)}$, $\mu_c \simeq \mu_{c,\,\text{sph}}+\mu_c^{(1)}$. The densities $\mu_s^{(1)}$, $\mu_{c,\,\text{sph}}$ and $\mu_c^{(1)}$ are given, approximately, by

$$\mu_s^{(1)}(y) = 2D\int(I-K_{\text{sph}})^{-1}(\alpha(y),\,\alpha(z))\left[\int_{S_h}\frac{\partial L_\infty(z,\,x,\,0)}{\partial n(x)}\mu_{\text{sph}}(x)\,dS(x)-\int_{S_c}L_\infty(z,\,x,\,0)\mu_{c,\,\text{sph}}(x)\,dS(x)\right]d\alpha(z)$$

$$=\mu_{s,\,S_h}^{(1)}(y)+\mu_{s,\,S_c}^{(1)}(y), \tag{13}$$

where the subscript S_h in $\mu_{s,\,S_h}^{(1)}$ indicates that it comes from an integration over S_h and so on for the others,

$$\mu_{c,\,\mathrm{sph}}(y) = \frac{2Dc}{a} + \left(a\frac{\partial}{\partial n(y)} + b\right)\frac{2D}{a}T_{\mathrm{sph}}(y), \tag{14}$$

$$\mu_c^{(1)}(y) = \left(a\frac{\partial}{\partial n(y)} + b\right)\left(\frac{2D}{a}\int_{S_{\mathrm{sph}}}\frac{\partial L_\infty(y,\,z,\,0)}{\partial n(z)}\mu_s^{(1)}(z)\,dS(z)\right.$$

$$\left. + \frac{2D}{a}\int_{S_c} L_\infty(y,\,z,\,0)\mu_{c,\,\mathrm{sph}}(z)\,dS(z) - \frac{2D}{a}\int_{S_h}\frac{\partial L_\infty(y,\,z,\,0)}{\partial n(z)}\mu_{\mathrm{sph}}(z)\,dS(z)\right) \tag{15}$$

with $\mu_c^{(1)}(y) = \mu_{c,\,S_{\mathrm{sph}}}^{(1)}(y) + \mu_{c,\,S_c}^{(1)}(y) + \mu_{c,\,S_h}^{(1)}(y)$. The MFPT function T in (12) is approximated by

$$T(x) \simeq T_{\mathrm{sph}}(x) + T^{(1)}(x), \tag{16}$$

where $T^{(1)}$ is given for every x inside Ω by

$$T^{(1)}(x) = \int_{S_{\mathrm{sph}}}\frac{\partial L_\infty(x,\,y,\,0)}{\partial n(y)}\mu_s^{(1)}(y)\,dS(y) + \int_{S_c} L_\infty(x,\,y,\,0)\mu_{c,\,\mathrm{sph}}(y)\,dS(y) - \int_{S_h}\frac{\partial L_\infty(x,\,y,\,0)}{\partial n(y)}\mu_{\mathrm{sph}}(y)\,dS(y)$$

$$= T_{S_{\mathrm{sph}}}^{(1)}(x) + T_{S_c}^{(1)}(x) + T_{S_h}^{(1)}(x). \tag{17}$$

At zeroth order of the approximation, the contribution of the small surfaces S_c and S_h are entirely neglected and S_s coincides with S_{sph}. Then, the density μ_s in (9) equals μ_{sph}, while T equals T_{sph}. On the other hand, μ_c (although safely disregarded at zeroth order) equals $\mu_{c,\,\mathrm{sph}}$. The normal derivatives are meaningful as, even if the sizes of S_c and S_h are very small (actually, discarded at zeroth order), inner unit normal vectors and, hence, inner normal derivatives from inside the domain can be defined. One sees that, as $(S_c \cup S_h) \setminus S_s$ vanishes, the small corrections $\mu_s^{(1)}$, $\mu_c^{(1)}$ and $T^{(1)}$ also vanish. The computation of $\mu_s^{(1)}$, $\mu_c^{(1)}$ and $T^{(1)}$, through the above nontrivial approximations, has been reduced to quadratures. The small contributions $\mu_{s,\,S_h}^{(1)}$, $\mu_{c,\,S_h}^{(1)}$ and $T_{S_h}^{(1)}$ involve integrations over S_h and integrands given in terms of spherical coordinates. Then, they can be reduced to convergent series in terms of Legendre polynomials, which can be taken from an analysis for a different case in [18] (namely, the MFPT for certain mixed boundary conditions on a spherical surface: Dirichlet ones over almost that surface except for a small region over it with Neumann ones). However, each of the remaining contributions in $\mu_{s,\,S_c}^{(1)}$, $\mu_{c,\,S_{\mathrm{sph}}}^{(1)} + \mu_{c,\,S_c}^{(1)}$ and $T_{S_{\mathrm{sph}}}^{(1)} + T_{S_c}^{(1)}$ contain integrations and integrands involving spherical and cylindrical contributions and are far more difficult, requiring numerical integrations lying outside our scope here.

The special situation when $b = 0$ and $c = 0$, ie, an absorbing sphere traversed by a reflective cylinder, could also be treated, in principle, through the above integral equation approach. As r ceases to be sufficiently small, an increasing number of iterations would be required. It appears interesting to get some quantitative knowledge of the MFPT for the present geometry, at least for the case $b = 0$ and $c = 0$, for values of r not too small, even if quantitative comparisons to the above integral equation approach at low order (requiring certainly quite small r) are unreliable. Such a study for $b = c = 0$, and not too small r, will require numerical methods: see Section 5.

3. Reflective deformed hollow sphere with a spherical trap inside

In this section, employing the *Second Strategy*, a particle is moving inside a domain Ω bounded by an absorbing inner spherical surface S_D of radius r, and a reflective outer closed surface (not necessarily spherical) S_N, so that the surface S_D is entirely enclosed by S_N. This geometry is related to and constitutes some extension of various studies on narrow capture problems. See [21–23, 25–28] and references therein. A simple example of this type of domain occurs if S_N is a hollow sphere, see Figure 2.

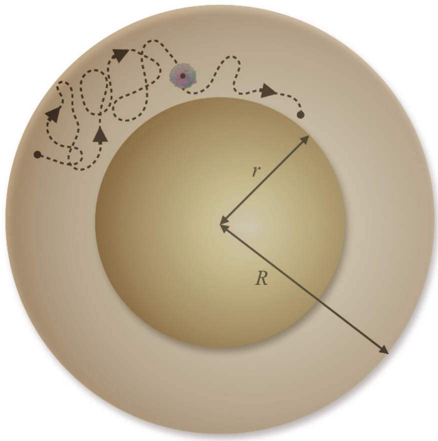

Figure 2. A reflective sphere of radius R with a concentric absorbing sphere of radius r

The particle is moving inside the domain Ω, far away from the outer surface, and, at some point, will reach the inner spherical boundary and leave it. Thus, the MFPT function T will be the solution of the Poisson equation with mixed Dirichlet and Neumann boundary conditions of type

$$D\Delta T(x) = -1 \quad \text{in } \Omega,$$

$$\lim_{x\to y} T(x) = 0 \quad \text{on } S_D, \tag{18}$$

$$\lim_{x\to y} \frac{\partial T}{\partial n}(x) = 0 \quad \text{on } S_N. \tag{19}$$

Let S denote the closed boundary surface of Ω defined as the union of the two disjoint closed surfaces S_D and S_N. The configuration of S, with an inner spherical surface trap S_D, gives rise to a narrow capture problem, as we shall see. The method below is different from those based on Green's functions. In short, the inverse of a certain operator (the actual counterpart of the operator $(I-K_{\text{sph}})^{-1}$ in Subsection 2.2 and Appendix A) does not exist for the actual boundary conditions and certain mathematical extension will be required to bypass that difficulty. The solution of such a problem will extend to the actual (in general, non-spherical and more difficult) surface S_N, the procedure in [17] (for Electrostatics) and in [18, Proposition 4.3] (for S_N a closed spherical surface concentric to S_D, like in Figure 2).

3.1 *Inhomogeneous integral equations including "conductor term"*

The MFPT function of a particle inside Ω is written from the outset as

$$T(x) = T_\infty(x) + \int_{S_D} \frac{\partial L_\infty(x, y, 0)}{\partial n(y)} \mu_D(y)\, dS(y) + \int_{S_N} L_\infty(x, y, 0) \mu_N(y)\, dS(y) + \mu_0 \int_{S_D} L_\infty(x, y, 0)\, dS(y), \tag{20}$$

where μ_0 is a non-vanishing constant. The structure of $\mu_0 \int_{S_D} L_\infty(x, y, 0)\, dS(y)$ will be necessary in order to solve the difficulties mentioned above. The developments below will confirm that. The last integral is the actual MFPT counterpart of what is named a "conductor term" in potential theory for Electrostatics [17]. We stress that the inner normal derivative at S_D throughout this section is opposite to the one in Appendix A: this is actually the origin of the difficulties to be met in this section. We shall discuss S_N later. One has

$$\int_{S_D} L_\infty(x, y, 0)\, dS(y) = \frac{r^2}{D|x|}.$$

From [18], including both Dirichlet and Neumann boundary conditions, the functions μ_D and μ_N satisfy the inhomogeneous system of linear integral equations of the second kind (which includes μ_0)

$$\mu_D(y) = -2DT_\infty(y) - 2D \int_{S_D} \frac{\partial L_\infty(y, z, 0)}{\partial n(z)} \mu_D(z)\, dS(z) - 2D \int_{S_N} L_\infty(y, z, 0) \mu_N(z)\, dS(z) - 2\mu_0 \frac{r^2}{|y|}, \tag{21}$$

$$\mu_N(y) = 2D \frac{\partial T}{\partial n}(x) \Big|_{x=y} \tag{22}$$

for y on S_D and S_N, respectively. We use the same T_∞ and L_∞. No additional equation is needed for μ_0.

3.2 *Justification of the Second Strategy*

For y on the inner boundary spherical surface S_D, ie $|y| = r$, let ${\mu_D}_l^m$ be defined by

$${\mu_D}_l^m = \mu_D(|y|)_l^m \equiv \int Y_l^m(\Omega_y)^* \mu_D(y)\, d\Omega_y \tag{23}$$

integrating over the whole solid angle Ω_y, and Y_l^m being the standard spherical harmonics (see [29]). We operate on equation (21) for μ_D so as to solve for all $\mu_D(|y|)_l^m$:

$$(I + K_{\text{sph}})\mu_D(y) = -2DT_\infty(y) - 2D \int_{S_N} L_\infty(y, z, 0) \mu_N(z)\, dS(z) - 2\mu_0 \frac{r^2}{|y|} \equiv \mu_{D,\, inh} \tag{24}$$

with the same K_{sph} as in Appendix A and Subsection 2.2, but here with the structure $(I + K_{\text{sph}})$ instead of $(I - K_{\text{sph}})$. That is due to the opposite sign of inner normal derivative on S_D, with respect to Subsection 2.2. This yields ($|y| = r$)

$$\int Y_l^{m*} \left(-2DT_\infty(y) - 2D \int_{S_N} L_\infty(y, z, 0) \mu_N(z) dS(z) - 2\mu_0 r \right) d\Omega_y = \left(1 - \frac{1}{2l+1} \right) {\mu_D}_l^m. \tag{25}$$

For $l = 0$, the previous equation (25) yields

$$\int Y_0^{0*} \left(-2DT_\infty(y) - 2D \int_{S_N} L_\infty(y, z, 0) \mu_N(z)\, dS(z) - 2\mu_0 r \right) d\Omega_y = 0 \tag{26}$$

and, for $l > 0$, it yields

$$\int Y_l^{m*} \left(-2DT_\infty(y) - 2D \int_{S_N} L_\infty(y, z, 0) \mu_N(z)\, dS(z) - 2\mu_0 r \right) d\Omega_y = \frac{2l}{2l+1} {\mu_D}_l^m. \tag{27}$$

There is a difficulty for $l = 0$, clearly. Previous equations (24), (25), (26) and (27) imply that $(I + K_{\text{sph}})^{-1}$ does not exist. In spite of that, equation (26) enables the determine μ_0 in terms of μ_N. At this stage, we appreciate the importance of having included the non-vanishing "conductor term" containing μ_0. Then, the equation (27) provides all ${\mu_D}_l^m$ for $l > 0$ in terms of μ_N and μ_0. If $\mu_0 = 0$ from the outset, then equation (26) would have become an additional constraint on μ_N which would be impossible to satisfy. Then, ${\mu_D}_0^0$ does not contribute to (24).

Stated differently, equation (24) reads

$$\mu_D = -K_{\text{sph}} \mu_D + \mu_{D,\, inh}.$$

Assume first that μ_0 does not satisfy (26). Then, the operator $-K_{\text{sph}}$ would have a non-zero eigenvalue equal to 1, with non-vanishing eigenfunction ψ, thereby preventing the inverse $(I + K_{\text{sph}})^{-1}$ from existing. Alternatively, if $\mu_{D,\,1}$ would be a solution of equation (24) as it stands, so would be $\mu_{D,\,2} = \mu_{D,\,1} + \lambda\,\psi$, for any real constant λ, that is, equation (24) would not have a unique solution. Now, assume that μ_0 does satisfy (26). Then, the inclusion of the "conductor term" suppresses any component proportional to ψ, as the resulting $\mu_{D,\, inh}$ has zero component proportional to the latter, by virtue of (26). In the subspace of functions orthogonal to ψ, the operator $(I + K_{\text{sph}})^{-1}$ exists: such a subspace corresponds to all $l > 0$. Equivalently, after the inclusion of the "conductor term" with μ_0 satisfying (26), equation (24) has a unique solution (in the subspace of functions orthogonal to ψ).

We now turn to equation (22) for μ_N, in order to check that, indeed, the contribution of ${\mu_D}_0^0$ in the former cancels out. In fact,

$$\begin{aligned}\mu_N(y) =& 2D \frac{\partial T_\infty}{\partial n}(y) + 2D \frac{\partial}{\partial n(y)} \left(\frac{1}{4\pi D} \int_{S_D} \frac{\partial}{\partial n(z)} \left[\sum_{l=0}^{+\infty} \frac{r_<^l}{r_>^{l+1}} \frac{4\pi}{2l+1} \sum_{m=-l}^{m=l} Y_l^m(\Omega_y) [Y_l^m(\Omega_z)]^* \mu_D(z) \right] dS(z) \right. \\ & \left. + \int_{S_N} L_\infty(y, z, 0) \mu_N(z)\, dS(z) + \mu_0 \int_{S_D} L_\infty(y, z, 0)\, dS(z) \right).\end{aligned} \tag{28}$$

The application of $\frac{\partial}{\partial n}$ implies that, as $|y|$ on S_N is greater than r, the contribution of $l = 0$, and, hence, that of ${\mu_D}_0^0$, vanishes identically. Then, only ${\mu_D}_l^m$ for $l > 0$ contribute in equation (28).

There still remains to check that the contribution of ${\mu_D}_0^0$ also disappears in the MFPT function. For that purpose, we recast the MFPT function in (20) as

$$T(x) = T_\infty(x) + \frac{1}{4\pi D}\int_{S_D}\frac{\partial}{\partial n(y)}\left[\sum_{l=0}^{+\infty}\frac{r_<^l}{r_>^{l+1}}\frac{4\pi}{2l+1}\sum_{m=-l}^{m=l}Y_l^m(\Omega_x)[Y_l^m(\Omega_y)]^*\mu_D(y)\right]dS(y)+$$

$$+\int_{S_N}L_\infty(x,\,y,\,0)\mu_N(y)dS(y)+\mu_0\int_{S_D}L_\infty(x,\,y,\,0)\,dS(y). \tag{29}$$

Again, the use of the partial derivative $\frac{\partial}{\partial n}$ implies that the contribution of $l=0$ vanishes identically when $|x|$ greater than r, and only ${\mu_D}_l^m$ for $l>0$ contribute in (29). The fact that ${\mu_D}_0^0$ does not contribute constitutes an important consistency condition. The non-vanishing ${\mu_D}_0^0$ remains undetermined, but this poses no problem, as shown.

3.3 *Modified integral equations for density functions*

Let S_N be the union of two open surfaces: $S_{N,\,1}$ and $\tilde{S}_N$. $S_{N,\,1}$ is a large part of a full spherical surface $S_{N,\,\mathrm{sph}}$ having radius $R>r$ and concentric with S_D. $\tilde{S}_N$ is a small non-spherical open surface (having an arbitrary shape). Let $S_{N,\,\mathrm{sph},\,2}$ be the small open part of $S_{N,\,\mathrm{sph}}$ such that the union of $S_{N,\,1}$ and $S_{N,\,\mathrm{sph},\,2}$ is just $S_{N,\,\mathrm{sph}}$. Since the dependences of L_∞ and $\frac{\partial L_\infty}{\partial n}$ on y are explicit, the right-hand side of (22) enables us to define μ_N on $S_{N,\,\mathrm{sph},\,2}$. Then, μ_N is defined (besides on $\tilde{S}_N$) on the whole $S_{N,\,\mathrm{sph}}$ (a similar extension was carried out in Subsection 2.2). This enables us to define the following integral, for compactness, as

$$\int_{\delta S_N}L_\infty\mu_N dS \equiv \int_{\tilde{S}_N}L_\infty\mu_N dS - \int_{S_{N,\,\mathrm{sph}}}L_\infty\mu_N dS$$

to be used in (20), (21) and (22). For y on $S_{N,\,\mathrm{sph}}$ ($|y|=R$), let

$${\mu_N}_l^m = \mu_N(|y|)_l^m \equiv \int Y_l^m(\Omega_y)^*\mu_N(y)d\Omega_y,$$

and integrate (21) and (22) over the whole solid angle. For y on S_D, equations (26) and (27) can be recast as

$$\int Y_0^{0*}\left(2DT_\infty(y)+2D\left(\int_{\delta S_N}L_\infty\mu_N dS\right)d\Omega_y\right)+4\sqrt{\pi}\mu_0 r+2\mu_{N0}^0R=0 \tag{30}$$

and

$$\int Y_l^{m*}\left(-2D\int_{\delta S_N}L_\infty(y,\,z,\,0)\mu_N(z)\,dS(z)\right)d\Omega_y-\frac{2}{2l+1}\frac{r^l}{R^{l-1}}\mu_{Nl}^m=\frac{2l}{2l+1}{\mu_D}_l^m. \tag{31}$$

One also gets, for y on $S_{N,\,\mathrm{sph}}$,

$$0=\int Y_0^{0*}2D\frac{\partial}{\partial n}\bigg|_{x=y}\left(T_\infty+\int_{\delta S_N}L_\infty\mu_N dS\right)d\Omega_y+\frac{4\sqrt{\pi}r^2}{R^2}\mu_0 \tag{32}$$

and, for $l > 0$,

$$\mu_{Nl}^{m} = \frac{2l+1}{2l} \int Y_l^{m*} 2D \frac{\partial}{\partial n}\bigg|_{x=y} \left(\int_{\delta S_N} L_\infty \mu_N dS \right) d\Omega_y + \frac{(l+1) r^{l+1}}{R^{l+2}} \mu_{Dl}^{m}. \tag{33}$$

Notice that, equations (30) and (32) give μ_0 and μ_{N0}^{0} while equations (31) and (33) give μ_{Dl}^{m} and μ_{Nl}^{m}, for $l > 0$, all in terms of $\int_{\delta S_N} L_\infty \mu_N dS$. The latter has been characterized above. For that purpose, use should also be made of (22) for z on $\tilde{S}_N$ and $S_{N,\,\mathrm{sph},\,2}$, which also makes sense by virtue of the above extension for z on $S_{N,\,\mathrm{sph},\,2}$. Such a use will not be necessary as long as one restricts to low-order computations, as discussed below.

In case that S_N coincides with the full spherical surface $S_{N,\,\mathrm{sph}}$, so that $\int_{\delta S_N} L_\infty \mu_N dS$ is absent, some computations yield ${\mu_D}_l^m = 0$, ${\mu_N}_l^m = 0$ for $l \geq 1$ and any m, and

$$\mu_0 = -\frac{R^3}{3r^2}, \qquad \mu_N = \frac{\mu_{No}^{0}}{\sqrt{4\pi}} = \frac{1}{3}\left(\frac{R^2}{r} + \frac{r^2}{2R} \right) \tag{34}$$

so that

$$T(x) = \frac{1}{D}\left(\frac{r^2 - |x|^2}{6} + \frac{R^3}{3r} - \frac{R^3}{3|x|} \right), \tag{35}$$

in agreement with [18]. It is important to notice that, for fixed R all μ_0, μ_N and T become larger in magnitude the smaller r is: this is interpreted as a signal of narrow escape of the Brownian particle towards the centre of S_D. In this case, the MFPT T does display the (short-distances) singularity at $r = 0$ in a simple way. In case that $\tilde{S}_N$ and $S_{N,\,\mathrm{sph},\,2}$ be small perturbations of the explicitly solvable case in equation (34), so that one can restrict to the lowest order correction, μ_N on δS_N can be approximated by $\frac{1}{3}\left(\frac{R^2}{r} + \frac{r^2}{2R} \right)$. This is meaningful provided that, for fixed R and (small) r, the contributions of $\tilde{S}_N$ and $S_{N,\,\mathrm{sph},\,2}$ be adequately smaller than those for $S_N = S_{N,\,\mathrm{sph}}$, as given in (34). This, in turn, occurs, if, semiquantitatively, $(R/r) \times$ (solid angle of $\tilde{S}_N$, as "seen" from the center of $S_D) \ll 1$. Then the corresponding system for μ_0, all μ_{Dl}^{m} for $l > 0$ and μ_{Nl}^{m} $l \geq 0$ is straightforward to solve.

4. Transmissible sphere with an absorbing thin cylinder trap

In this section, we also consider the same domain Ω, with the same boundary surface S, displayed in Figure 1 (the radius r of the thin cylinder being supposed much smaller than h_1), but with different boundary conditions which will make the present case quite different from that in Section 2. Now, the particle is moving inside Ω and we assume that the outer spherical surface S_s is transmissible, so there are some particles that may leave the domain while others may come in through the outer boundary. On the other hand, the inner cylindrical surface S_c is absorbing, ie the particle, at some instant, will leave the domain through it. In this way, the MFPT function T satisfies the Poisson equation with mixed Robin and Dirichlet boundary conditions of type

$$D\Delta T(x) = -1 \;\text{ in } \Omega,$$

$$a \lim_{x \to y} \frac{\partial T}{\partial n}(x) + b \lim_{x \to y} T(x) + c = 0 \qquad \text{on } S_s,$$

$$\lim_{x \to y} T(x) = 0 \qquad \text{on } S_c,$$

whenever $a \neq 0$, b and c are real constants. Important differences occur depending on b. We shall treat only the case $b \neq 0$ through the integral equation approach. We anticipate that the case $b = 0$ will meet difficulties in the integral equation approach, and it will be studied (also with $c = 0$, for simplicity) numerically in Section 5.

4.1 *Case b ≠ 0: Integral equations*

The MFPT function T is characterized, for every $x \in \Omega$, by

$$T(x) = T_\infty(x) + \int_{S_c} \frac{\partial L_\infty(x,\, y,\, 0)}{\partial n(y)} \mu_c(y) dS(y) + \int_{S_s} L_\infty(x,\, y,\, 0) \mu_s(y) dS(y) \tag{36}$$

with the same T_∞ and L_∞ as in the previous sections. The densities μ_c and μ_s are defined in S_c and S_s, respectively, as the solution of the inhomogeneous system of linear integral equations

$$\mu_c(y) = -2D \left(T_\infty(y) + \int_{S_c} \frac{\partial L_\infty(y,\, z,\, 0)}{\partial n(z)} \mu_c(z) dS(z) + \int_{S_s} L_\infty(y,\, z,\, 0) \mu_s(z) dS(z) \right) \tag{37}$$

$$\mu_s(y) = \left(a \frac{\partial}{\partial n} + b \right) \frac{2D}{a} T_\infty(y) + \frac{2D}{a} \left(a \frac{\partial}{\partial n(y)} + b \right) \left(\int_{S_s} L_\infty(y,\, z,\, 0) \mu_s(z)\, dS(z) \right.$$

$$\left. + \int_{S_c} \frac{\partial L_\infty(y,\, z,\, 0)}{\partial n(z)} \mu_c(z)\, dS(z) \right) + \frac{2Dc}{a}. \tag{38}$$

The above three equations for T, μ_c and μ_s hold without approximations. For a general x, one has in cylindrical coordinates $x = (\rho,\, \varphi,\, z)$. Like in Section 2, particle migration is naturally assumed to have cylindrical symmetry around the cylinder axis. Consequently, T, μ_c and μ_s will be independent of angles φ about the cylinder axis. The physical dimensions (dim) of the various relevant quantities are (L denoting length): dim $T = L^2/D$, dim $L_\infty = 1/LD$, dim $\mu_s = L$, dim $\mu_c = L^2$, dim $(a/b) = L$, dim $(c/b) = L^2/D$, and dim $(cD/bR) = L$. The density $\mu_c(z)$ will be expanded into a Fourier series in $-h_1 < z < h_1$ as

$$\mu_c(z) = \frac{\mu_{c,\,0}}{2} + \sum_{n=-\infty,\, n \neq 0}^{+\infty} \mu_{c,\,n} e^{izn\pi/h_1}. \tag{39}$$

At this stage, we proceed as in Subsection 2.2, with a similar full spherical surface S_{sph}, an open "beret" S_h with $S_{\text{sph}} = S_s \cup S_h$ and extension of the right-hand side of (38) to any point on S_{sph}. This enables us to define μ_s on S_h and, hence, over the whole S_{sph}. So, we implement the First strategy, which will turn out to suffice. By adding and subtracting surface integrals like in Subsection 2.2, equations (37) and (38) become

$$\mu_c(y) = -2D\left(T_\infty(y) + \int_{S_c} \frac{\partial L_\infty(y, z, 0)}{\partial n(z)} \mu_c(z) dS(z) + \int_{S_{\text{sph}}} L_\infty(y, z, 0)\mu_s(z) dS(z) - \int_{S_h} L_\infty(y, z, 0)\mu_s(z)\, dS(z)\right) \quad (40)$$

and

$$\mu_s(y) = \left(a\frac{\partial}{\partial n} + b\right)\frac{2D}{a}T_\infty(y) + \frac{2Dc}{a} + \frac{2D}{a}\left(a\frac{\partial}{\partial n(y)} + b\right)\left(\int_{S_{\text{sph}}} L_\infty(y, z, 0)\mu_s(z)\, dS(z)\right.$$

$$\left. + \int_{S_c} \frac{\partial L_\infty(y, z, 0)}{\partial n(z)} \mu_c(z)\, dS(z) - \int_{S_h} L_\infty(y, z, 0)\mu_s(z)\, dS(z)\right). \quad (41)$$

At this point, we extend the developments in Subsection 2.2 and recall the developments in Appendix A, for the spherical surface with Robin boundary conditions. Then, μ_c in (40) (using (64)) and μ_s in (41) (using (65) and (66)) become

$$\mu_c(y) = -2D\left(T_{Rob}(y) + \int_{S_{\text{sph}}} L_\infty(y, z, 0)(\mu_s(z) - \mu_{Rob}(z)) dS(z)\right.$$

$$\left. + \int_{S_c} \frac{\partial L_\infty(y, z, 0)}{\partial n(z)} \mu_c(z) dS(z) - \int_{S_h} L_\infty(y, z, 0)\mu_s(z) dS(z)\right) \quad (42)$$

$$\mu_s(y) = \int (I - K_{Rob})^{-1}(\alpha(y), \alpha(u))\frac{2D}{a}\left(a\frac{\partial}{\partial n(u)} + b\right)\left(\int_{S_c} \frac{\partial L_\infty(u, z, 0)}{\partial n(z)} \mu_c(z) dS(z)\right.$$

$$\left. - \int_{S_h} L_\infty(u, z, 0)\mu_s(z) dS(z)\right) d\alpha(u) + \mu_{Rob}(y) \quad (43)$$

where μ_{Rob} and T_{Rob} are given in Appendix A. As r, radius of S_c, vanishes, it is reasonable that $\mu_s(y)$ tends to $\mu_{Rob}(y)$ for consistency. We focus here on μ_c (with y on S_c), leaving μ_s (with y on S_s) to the next subsection. We apply $\int_{-h_1}^{+h_1}$ to (42) (thereby proceeding to $\mu_{c,0}$), operate in $\int_{S_c} \frac{\partial L_\infty(y, z, 0)}{\partial n(z)}$ using (71), use (39) and cancel out two contributions equal to $\mu_{c,0}$. Then, μ_c in (42) yields

$$\mu_{c,0}\frac{r}{h_1}\left(\int_0^{+\infty} J_0(\kappa r) \left.\frac{\partial J_0(\kappa\rho')}{\partial \rho'}\right|_{\rho'=r} \frac{1 - e^{-2h_1\kappa}}{\kappa^2}\, d\kappa\right)$$

$$= \frac{r}{h_1}\left(\sum_{n=-\infty,\, n\neq 0}^{+\infty} \mu_{c,n}(-1)^n \int_0^{+\infty} J_0(\kappa r) \left.\frac{\partial J_0(\kappa\rho')}{\partial \rho'}\right|_{\rho'=r} \frac{2(1 - e^{-2h_1\kappa})}{\kappa^2 + (n\pi/h_1)^2}\, d\kappa\right)$$

$$
-\frac{2D}{h_1}\int_{-h_1}^{+h_1} dz\left(T_{Rob}(y)+\int_{S_{\rm sph}} L_\infty(y,\, z,\, 0)(\mu_s(z)-\mu_{Rob}(z))dS(z)-\int_{S_h} L_\infty(y,\, z,\, 0)\mu_s(z)dS(z)\right), \tag{44}
$$

and for $n \neq 0$

$$
\begin{aligned}
\mu_{c,\,n} = & \frac{r(-1)^n}{h_1}\left(\mu_{c,\,0}\int_0^{+\infty} J_0(\kappa r)\,\frac{\partial J_0(\kappa\rho')}{\partial\rho'}\bigg|_{\rho'=r}\frac{1-e^{-2h_1\kappa}}{\kappa^2+(n\pi/h_1)^2}d\kappa\right.\\
& \left.+\sum_{\substack{n'=-\infty\\ n'\neq 0}}^{+\infty}\mu_{c,\,n}(-1)^{n'}\int_0^{+\infty} J_0(\kappa r)\,\frac{\partial J_0(\kappa\rho')}{\partial\rho'}\bigg|_{\rho'=r}\frac{2(1-e^{-2h_1\kappa})(\kappa^2-nn'(\pi/h_1)^2)}{(\kappa^2+(n\pi/h_1)^2)(\kappa^2+(n'\pi/h_1)^2)}d\kappa\right)\\
& -\frac{2D}{h_1}\int_{-h_1}^{+h_1} e^{-i(n\pi z/h_1)}dz\left(T_{Rob}(y)+\int_{S_{\rm sph}} L_\infty(y,\, z,\, 0)(\mu_s(z)-\mu_{Rob}(z))dS(z)-\int_{S_h} L_\infty(y,\, z,\, 0)\mu_s(z)dS(z)\right).
\end{aligned} \tag{45}
$$

So, use is made in this subsection of the properties summarized in Appendix B.

4.2 *Case $b \neq 0$: Approximate solutions and signal of narrow escape*

We now proceed to the lowest approximation. We drop contributions of orders $\int_{S_h}$ and $\mu_s(z)-\mu_{Rob}(z)$ in $\mu_{c,\,0}$ and $\mu_{c,\,n}$. For $n=0$, we may approximate $\mu_{c,\,0}\simeq\mu_{c,\,0}^{(0)}$ with

$$
\mu_{c,\,0}^{(0)} = \left(\int_0^{+\infty} J_0(\kappa r)\,\frac{\partial J_0(\kappa\rho')}{\partial\rho'}\bigg|_{\rho'=r}\frac{1-e^{-2h_1\kappa}}{\kappa^2}\,d\kappa\right)^{-1}\left(-\frac{2D}{r}\int_{-h_1}^{+h_1} dz\, T_{Rob}(y)\right).
$$

The integral over κ contained in $\mu_{c,\,0}^{(0)}$ does not vanish as $r\to 0$, as an analysis of the integrand indicates. For $n\neq 0$, we may approximate $\mu_{c,\,n}$ in (45) by

$$
\mu_{c,\,n}\simeq\mu_{c,\,n}^{(0)} = -\frac{2D}{h_1}\int_{-h_1}^{+h_1} 1dz\, T_{Rob}(y)\left(e^{-i(n\pi z/h_1)}+(-1)^n\frac{\displaystyle\int_0^{+\infty} J_0(\kappa r)\,\frac{\partial J_0(\kappa\rho')}{\partial\rho'}\bigg|_{\rho'=r}\frac{(1-e^{-2h_1\kappa})}{(\kappa^2+(n\pi/h_1)^2)}d\kappa}{\left(\displaystyle\int_0^{+\infty} J_0(\kappa r)\,\frac{\partial J_0(\kappa\rho')}{\partial\rho'}\bigg|_{\rho'=r}\kappa^{-2}(1-e^{-2h_1\kappa})d\kappa\right)}\right).
$$

The integral $\displaystyle\int_0^{+\infty} J_0(\kappa r)\,\frac{\partial J_0(\kappa\rho')}{\partial\rho'}\bigg|_{\rho'=r}\frac{(1-e^{-2h_1\kappa})}{(\kappa^2+(n\pi/h_1)^2)}d\kappa$ contained in $\mu_{c,\,n}^{(0)}$ does not vanish as $r\to 0$, through similar arguments.

Similarly, we may approximate $\mu_s(y)\simeq\mu_s^{(0)}(y)+\mu_s^{(1)}(y)$ with $\mu_s^{(0)}(y)=\mu_{Rob}(y)$ and using equation (71). On S_{sph}, u has spherical coordinates $(r,\, \theta_u,\, \phi_u)$ and its third component is $z_u = r\cos\theta_u$. Then

$$\mu_s^{(1)}(y) = -\int d\alpha(u)(I-K_{Rob})^{-1}(\alpha(y),\, \alpha(u))\frac{2D}{a}\left(a\frac{\partial}{\partial n(u)}+b\right)\times$$

$$\left(\frac{\displaystyle\int_0^{+\infty} J_0(\kappa\rho)\,\frac{dJ_0(\kappa\rho')}{d\rho'}\bigg|_{\rho'=r}\frac{2-e^{-\kappa(h_1-z_u)}-e^{-\kappa(z_u+h_1)}}{\kappa}\,d\kappa}{\displaystyle 2\int_0^{+\infty} J_0(\kappa r)\,\frac{\partial J_0(\kappa\rho')}{\partial\rho'}\bigg|_{\rho'=r}\frac{1-e^{-2h_1\kappa}}{\kappa^2}\,d\kappa}\int_{-h_1}^{+h_1} dz T_{Rob}(y)\right). \tag{46}$$

We emphasize that $\mu_s^{(1)}(y)$ tends to 0 if r vanishes, as it should be for consistency. This follows from the fact that, as ρ corresponds to a point on S_s, the integral $\int_0^{+\infty} J_0(\kappa\rho)\,\frac{dJ_0(\kappa\rho')}{d\rho'}\Big|_{\rho'=r}\frac{2-e^{-\kappa(h_1-z_u)}-e^{-\kappa(z_u+h_1)}}{\kappa}\,d\kappa$ tends to 0 if r vanishes, as an analysis of the integrand shows.

On the other hand, through similar arguments, we derive the exact representation

$$T(x) = T_{Rob}(x) + \int_{S_c}\frac{\partial L_\infty(x,\, y,\, 0)}{\partial n(y)}\mu_c(y)dS(y) + \int_{S_{\rm sph}} L_\infty(x,\, y,\, 0)(\mu_s(y)$$

$$-\mu_{Rob}(y))dS(y) - \int_{S_h} L_\infty(x,\, y,\, 0)\mu_s(y)dS(y). \tag{47}$$

This, in turn, can be approximated as $T(x)\simeq T^{(0)}(x)+T^{(1)}(x)$, with $T^{(0)}(x) = T_{Rob}(x)$ and (p and z_x being the cylindrical coordinates of x)

$$T^{(1)}(x) = -\frac{\displaystyle\int_0^{+\infty} J_0(\kappa\rho)\frac{dJ_0(\kappa r)}{d\rho'}\bigg|_{\rho'=r}\frac{2-e^{-\kappa(h_1-z_x)}-e^{-\kappa(z_x+h_1)}}{\kappa}\,d\kappa}{\displaystyle 2\int_0^{+\infty} J_0(\kappa r)\,\frac{\partial J_0(\kappa\rho')}{\partial\rho'}\bigg|_{\rho'=r}\frac{1-e^{-2h_1\kappa}}{\kappa^2}\,d\kappa}\int_{-h_1}^{+h_1} dz\; T_{Rob}(y). \tag{48}$$

Through a study similar to that for $\mu_s^{(1)}(y)$, both the integral over κ in the numerator in $T^{(1)}(x)$ and, hence, $T^{(1)}(x)$ approach 0 if r vanishes, as it should also be for consistency. The contribution $-\frac{2D}{r}\int_{-h_1}^{+h_1} dz\; T_{Rob}(y)$ in $\mu_{c,\,0}^{(0)}$, large due to $\frac{1}{r}$, can be regarded as a (weak) signal of a narrow capture situation. Notice that, only $\mu_{c,\,0}^{(0)}$ increase as the cylinder becomes thinner, while none of $\mu_{c,\,n}^{(0)}$ ($n\neq 0$) and $\mu_s^{(0)}$ display such behaviour. The MFPT $T^{(0)}$ does not exhibit the short-distance singularity $\left(\frac{1}{r}\right)$ as r vanishes, which is smoothed out by the spatial integration $\int_{S_c} dS(y)$ in (47). Thus, the narrow escape for the sphere traversed by a cylinder is weaker than the one for the hollow sphere in Section 3. Anyway, the integral equation approach has enabled the display of some weak signal of narrow capture towards the thin cylinder. The first-order correction is obtained by following the procedure in Subsection 2.3. Detail is omitted. Since μ_{Rob} and T_{Rob} diverge as $b\to 0$ (see equations (67) and (68)), the developments in this section do not hold if $b=0$. This does not prevent the MFPT from existing and being well defined for $b=0$ but , in such a case, an analytical approach lies outside our scope here. We shall proceed to a numerical study of it in Section 5.

5. Numerical solutions in the unit sphere traversed by a thin cylinder

In this section, computational studies are carried out for the MFPT corresponding to the geometries in Sections 2 and 4. For that purpose, we shall recast the Poisson equation into a dimensionless form. We scale $x = lx_d$ and $T = (l^2/D)T_d$, where l is a suitable unit of length and the new position vector x_d and T_d are dimensionless. Then, $D\Delta T(x) = -1$ is recast into the dimensionless form $\Delta_d T_d(x_d) = -1$, where Δ_d is the Laplacian with respect to x_d. To fix the ideas, D/a_0 can be taken about $2.2\times 10^{-9} m^2 s^{-1}$ (the diffusion coefficient of water at room conditions). a_0 (dimensionless) is about 10^{-2} for a globular protein and decreases as the radius of the Brownian particle increases (roughly, as 1/(radius of the particle)). l could be chosen, say, between one mm and one μm. Throughout this section, we consider dimensionless quantities, but the subscript d will be omitted, with the understanding that $T_d = T$ and $x_d = x$ are dimensionless.

Let us consider the domain Ω, given in Figure 1, formed by a unit sphere centered at the origin traversed by a cylinder with radius $r = \frac{1}{5}$. We anticipate that the actual cylinder radius $r = \frac{1}{5}$ is not sufficiently small to compare with possible numerical results following from the analytical studies to first-order in Subsection 2.3. First, assume that the Brownian particle moves inside an absorbing unit sphere traversed by a reflective thin cylinder, so that the MFPT function is the solution of the problem

$$\Delta T(x) = -1 \ \text{ in } \Omega, \tag{49}$$

$$T = 0 \ \text{ on } S_s, \tag{50}$$

$$\frac{\partial T}{\partial n} = 0 \ \text{ on } S_c, \tag{51}$$

where the homogeneous Dirichlet boundary condition is on the sphere, and the Neumann one on the cylinder. Since our domain is symmetric respect to the plane $Y = 0$, we represent, in Figure 3a, the numeric MFPT function T solution of the Poisson problem, defined in cylindrical coordinates (ρ, z), where ρ stands for the radial distance from the cylinder axis, and z the vertical (ie the third cartesian) coordinate, when $\frac{1}{5} \le \rho \le 1$ and $-1 \le z \le 1$. Figure 3a displays, at fixed ρ, how the MFPT decreases as $|z|$ tends to 1, ie the MFPT decreases when the particle approaches the circumference along the intersection between the sphere and the cylinder. Moreover, at fixed z, the MFPT decreases as ρ tends to 1, ie the mean time decreases when the particle approaches the absorbing unit sphere boundary. Along $z = 0$, in Figure 3b, the monotone profile highlights how an impermeable vessel delays encounters with the exit. In a cell-migration analogue (absorbing organ boundary, non-adhesive vessel), cells starting near the vessel axis experience longer residence times than those near the organ periphery.

Now, we assume that the Brownian particle moves inside a reflective unit sphere traversed by an absorbing thin cylinder. Then, the MFPT function is the solution of the Poisson equation (49) subject to the mixed Neumann-Dirichlet boundary conditions

$$\frac{\partial T}{\partial n} = 0 \ \text{ on } S_s, \tag{52}$$

$$T = 0 \ \text{ on } S_c, \tag{53}$$

precisely the Neumann boundary condition is on the sphere, and the Dirichlet one on the cylinder. One reason making this case particularly interesting is that it corresponds to $b = 0$ and $c = 0$, not covered by the previous integral equation approach in Section 4. Its numeric solution is plotted in Figure 4a in cylindrical coordinates (ρ, z) when $\frac{1}{5} \le \rho \le 1$ and

$-1 \leq z \leq 1$. Here the MFPT drops sharply near the absorbing cylinder and is largest near the reflective outer wall. Figure 4a displays, at fixed ρ, how the MFPT decreases as $|z|$ tends to 1, ie the MFPT decreases when the Brownian particle approaches the circumference along the intersection between the sphere and the cylinder. Besides, at fixed z, the MFPT decreases as the radius ρ tends to $\frac{1}{5}$, showing a narrow capture tendency that strengthens as the cylinder radius decreases. Biologically, a capturing/adhesive vessel yields fast encounters for cells near the vessel and delayed capture for cells near the organ boundary.

The numerical MFPT maps corroborate the theoretical trends. A reflective cylinder acts as a delay-inducing obstacle (as in Figure 3), whereas an absorbing cylinder produces a pronounced capture basin along the vessel, with minimal MFPT near $\rho = r$ (as in Figure 4).

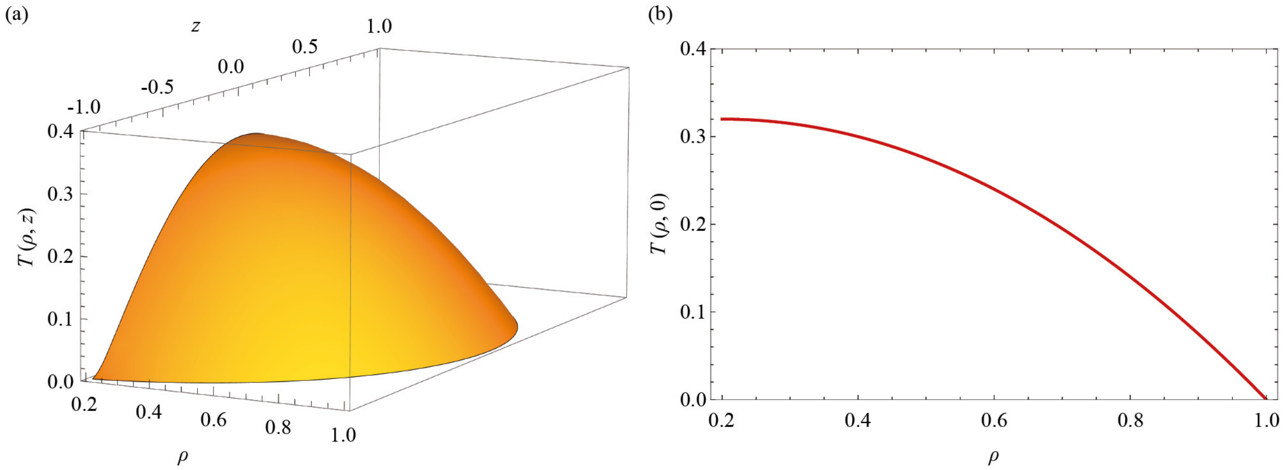

Figure 3. In the panel (a), the MFPT function T solution of (49), with absorbing boundary condition (50) on the unit spherical surface, and reflective boundary (51) on the cylindrical surface of radius $\frac{1}{5}$, defined in cylindrical coordinates $(\rho, z) \in [\frac{1}{5}, 1] \times [-1, 1]$. In the panel (b), the MFPT function when $z = 0$ and $\rho \in [\frac{1}{5}, 1]$

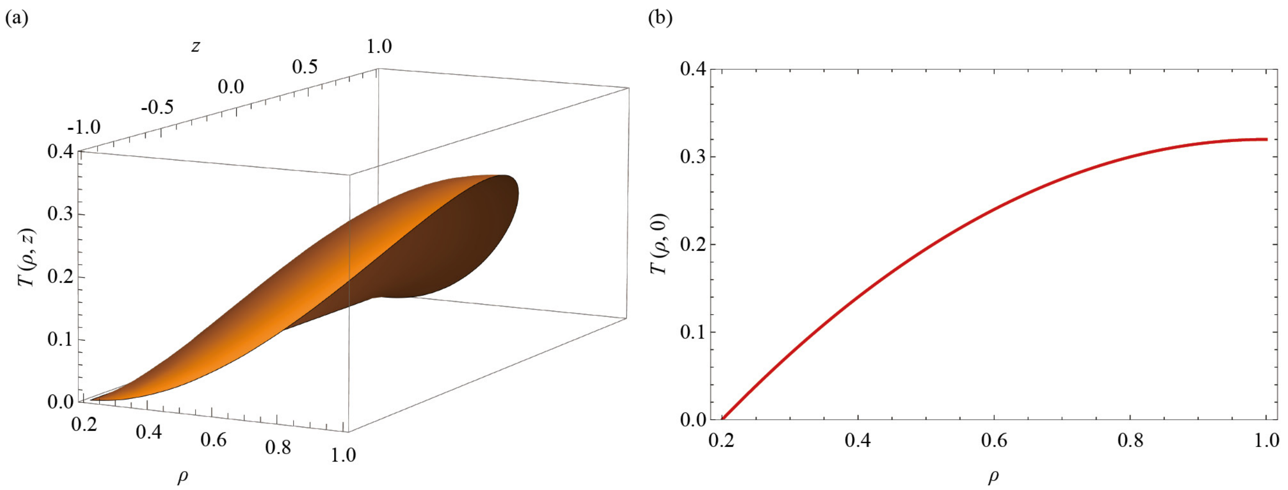

Figure 4. In the panel (a), the MFPT function T solution of (49), with reflective boundary condition (53) on the unit spherical surface, and absorbing boundary (52) on the cylindrical surface of radius $\frac{1}{5}$, defined in cylindrical coordinates $(\rho, z) \in [\frac{1}{5}, 1] \times [-1, 1]$. In the panel (b), the MFPT function when $z = 0$ and $\rho \in [\frac{1}{5}, 1]$

6. Conclusion and discussions

The passive Brownian motion of a particle in a fluid at rest is studied. The particle diffusion is considered in three-dimensional finite domains Ω bounded by closed surfaces S, which pose non-trivial boundary value problems. The mean first-passage time, satisfying the adjoint Poisson equation, characterizes the particle migration inside Ω and the possibility of reaching S. It provides an interesting alternative to the use of Green's functions.

Equations (1), (2) and (3) in Section 2, related ones in Section 4, and (18) and (19) in Section 3 (and simplifications and reformulations thereof) for other geometries, appear in the literature. What is different in the present work is the following. We have studied here the methodological characterization of the mean first-passage time, through suitable inhomogeneous linear integral equations for certain density functions on S, encoding the boundary conditions and extending potential theory for Electrostatics non-trivially. Dirichlet, Neumann and Robin boundary conditions are considered, as mixed boundary conditions (a genuine long-standing and open problem). The approach allows for possible approximations for the mean first-passage time, for suitable surfaces S which be small or controllable deformations of certain surfaces (spherical surfaces, concentric spherical surfaces, cylinders and some others). One virtue of such an integral equation approach is that, in principle, it displays situations with narrow escape, which has also motivated our theoretical analysis here.

The following intriguing conceptual issue may arise: for certain boundary conditions, the inhomogeneous linear integral equations, as directly formulated and as a consequence of the signs in inner normal derivatives, have no solutions. Fortunately, the addition of suitable "conductor" surface terms leads to other inhomogeneous linear integral equations which do have solutions. This is precisely what happens for a reflective deformed sphere with an absorbing spherical trap.

By following those strategies, the mean first-passage time for the following new surfaces has been analysed:

• absorbing sphere traversed by a transmissible thin cylinder, in Section 2, with *First Strategy* and no narrow escape,

• reflective deformed sphere with an absorbing spherical trap, in Section 3, with *Second Strategy* (including a "conductor" surface term): the mean first-passage time, has a short-distance singularity and a neat narrow escape

• transmissible sphere traversed by an absorbing thin cylinder, in Section 4, still with *First Strategy* and weak narrow escape .

Emphasis in Sections 2 and 4 has focused on displaying the crucial differences between geometries for a small radius of the cylinder, rather than on numerical computations for them.

We emphasize that for a transmissible sphere (Robin boundary condition) traversed by an absorbing thin cylinder (Section 4), the integral equation approach (*First Strategy*, without "conductor" surface terms), suffices to arrive at approximate solutions, with a weak, narrow escape, always with a finite mean first-passage time. This contrasts with the case in Section 3.

For the interest of providing quantitative information on the mean first-passage time for the geometry in Section 2 and 4 for simpler cases ($b = 0$ and $c = 0$), numerical computations based directly on the adjoint Poisson equations have also been carried out in Section 5:

• for an absorbing unit sphere traversed by a reflective cylinder, with radius r not sufficiently small to allow for a direct comparison with the low-order analytical computations in Section 2,

• for a reflective unit sphere traversed by an absorbing thin cylinder, a particularly interesting case because it corresponds to a situation, not covered by the integral equation approach in Section 4.

Acknowledgement

This work was partially supported by Ministerio de Ciencia, Innovación y Universidades (MICIU, Spain), Agencia Estatal de Investigación (AEI, Spain, MCIN/AEI/10.13039/501100011033), and European Regional Development Fund (ERDF, A way of making Europe) through Grant no. PID2022-136374NB-C21.

Conflict of interest

The authors declare no competing financial interest.

References

[1] Bénichou O, Voituriez R. From first-passage times of random walks in confinement to geometry-controlled kinetics. *Physics Reports*. 2014; 539: 225.

[2] Bénichou O, Voituriez R. Narrow-escape time problem: Time needed for a particle to exit a confining domain through a small window. *Physical Review Letters*. 2008; 100: 168105.

[3] Bressloff PC, Earnshaw BA, Ward MJ. Diffusion of protein receptors on a cylindrical dendritic membrane with partially absorbing traps. *SIAM Journal on Applied Mathematics*. 2008; 68(5): 1223-1246.

[4] Condamin S, Bénichou O, Tejedor V, Voituriez R, Klafter J. First-passage times in complex scale-invariant media. *Nature*. 2007; 450: 77.

[5] Dahlenburg M, Pagnini G. Exact calculation of the mean first passage time of continuous-time random walks by nonhomogeneous Wiener-Hopf integral equations. *Journal of Physics A: Mathematical and Theoretical*. 2022; 55: 505003.

[6] Gilbert J, Cheviakov A. Global optimisation of the mean first passage time for narrow capture problems in elliptic domains. *European Journal of Applied Mathematics*. 2023; 34(6): 1269-1287.

[7] Grebenkov DS, Skvortsov AT. Mean first-passage time to a small absorbing target in an elongated planar domain. *New Journal of Physics*. 2020; 22: 113024.

[8] Guérin T, Levernier N, Bénichou O, Voituriez R. Mean first-passage times of non-Markovian random walkers in confinement. *Nature*. 2016; 534: 356-359.

[9] Iyaniwura S, Wong T, Macdonald CB, Ward MJ. Optimization of the mean first passage time in near-disk and elliptical domains in 2D with small absorbing traps. *SIAM Review*. 2021; 63(3): 525-555.

[10] Jacobs K. *Stochastic Processes for Physicists*. Cambridge, UK: Cambridge University Press; 2010.

[11] Mattos TG, Mejia-Monasterio C, Metzler R, Oshanin G. First passages in bounded domains: When is the first-passage time meaningful? *Physical Review E*. 2012; 86: 031143.

[12] Metzler R, Oshanin G, Redner S. *First-Passage Phenomena and Their Applications*. Singapore: World Scientific; 2014.

[13] Mutothya NM, Xu T. Mean first passage time for diffuse and rest search in a confined spherical domain. *Physica A: Statistical Mechanics and Its Applications*. 2021; 567: 125667.

[14] Redner S. *A Guide to First-Passage Processes*. Cambridge, UK: Cambridge University Press; 2007.

[15] Singer A, Schuss Z, Holcman D. Narrow escape and leakage of Brownian particles. *Physical Review E*. 2008; 78(5): 051111.

[16] Vaccario G, Antoine C, Talbot J. First-passage times in d-dimensional heterogeneous media. *Physical Review Letters*. 2015; 115: 240601.

[17] Kellogg OD. *Foundations of Potential Theory*. Berlin/Heidelberg, Germany; New York, NY, USA: Springer; 1967.

[18] Serrano H, Álvarez Estrada RF, Calvo GF. Mean first-passage time of cell migration in confined domains. *Mathematical Methods in the Applied Sciences*. 2023; 46(6): 7435-7453.

[19] Serrano H, Álvarez Estrada RF. Characterization of the mean first-passage time function subject to advection in annular like domains. *Mathematics*. 2023; 11(24): 4998.

[20] Serrano H, Álvarez Estrada RF. Review on some boundary value problems defining the mean first-passage time in cell migration. *Axioms*. 2024; 13(8): 537.

[21] Bressloff PC. Asymptotic analysis of target fluxes in the three-dimensional narrow capture problem. *Multiscale Modeling and Simulation*. 2021; 19(2): 612-632.

[22] Bressloff PC. The 3D narrow capture problem for traps with semipermeable interfaces. *Multiscale Modeling and Simulation*. 2023; 21(3): 1268-1298.

[23] Cheviakov AF, Ward MJ, Straube R. An asymptotic analysis of the mean first passage time for narrow escape problems. II The sphere. *Multiscale Modeling and Simulation*. 2010; 8(3): 836-870.

[24] Coombs D, Straube R, Ward MJ. Diffusion on a sphere with localized traps: Mean first passage time, eigenvalue asymptotics, and Fekete points. *SIAM Journal on Applied Mathematics*. 2009; 70(1): 302-332.

[25] Grebenkov DS, Rupprecht JF. The escape problem for mortal walkers. *The Journal of Chemical Physics*. 2017; 146: 084106.

[26] Holcman D, Schuss Z. The narrow escape problem. *SIAM Review*. 2014; 56(2): 213-257.

[27] Mangeat M, Rieger H. The narrow escape problem in a circular domain with radial piecewise constant diffusivity. *Journal of Physics A: Mathematical and Theoretical*. 2019; 52: 424002.

[28] Ridgway WJM, Cheviakov AF. Locally and globally optimal configurations of N particles on the sphere with applications in the narrow escape and narrow capture problems. *Physical Review E*. 2019; 100: 042413.

[29] Morse PM, Feshbach H. *Methods of Theoretical Physics. Part I and Part II*. New York, NY, USA: McGrawHill; 1953.

Appendix A. Spherical surface with either Dirichlet or Robin boundary condition

First, the MFPT for a diffusing particle inside a sphere Ω of radius R with an absorbing boundary S_{sph} will be reviewed by using the linear integral equation approach [18, Proposition 3.3]. So, our presentation of the integral equation approach for the geometries considered will be essentially self-contained. One starts with the Poisson equation in the sphere with a Dirichlet boundary condition of type

$$D\Delta T(x) = -1 \;\text{ in } \Omega,$$

$$\lim_{x\to y} T(x) = 0 \;\text{ on } S_{\text{sph}}, \tag{54}$$

whose solution is given by

$$T(x) = T_\infty(x) + \int_{S_{\text{sph}}} \frac{\partial L_\infty(x,\, y,\, 0)}{\partial n(y)} \mu(y)\, dS(y), \tag{55}$$

where the function μ satisfies the inhomogeneous linear integral equation of second kind

$$\mu(y) = -2DT_\infty(y) - 2D\int_{S_{\text{sph}}} \frac{\partial L_\infty(y,\, z,\, 0)}{\partial n(z)} \mu(z)\, dS(z). \tag{56}$$

Firstly, consider the standard spherical coordinates $y = (r,\, \theta,\, \varphi)$, with $r = |y|$, the solid angle $\alpha(y) = (\theta,\, \varphi)$, as well as the spherical harmonic functions $\{Y_l^m\}$ which satisfy the orthonormality property

$$\int [Y_l^m(\alpha(y))]^* Y_{l'}^{m'}(\alpha(y))\, d\alpha(y) = \delta_{l,\, l'}\delta_{m,\, m'} \tag{57}$$

with $d\alpha(y) = \sin\theta d\theta d\varphi$. Here, the integration over $\alpha(y)$ is carried out over the whole solid angle, so that $\delta_{l,\, l'} = 0$ for $l \neq l'$ while $\delta_{l,\, l} = 1$, and so on for $\delta_{m,\, m'}$. Then, for any x and y in Ω, take into account the following expansion

$$\frac{1}{|x-y|} = \sum_{l=0}^{+\infty} \frac{r_<^l}{r_>^{l+1}} \frac{4\pi}{2l+1} \sum_{m=-l}^{m=l} Y_l^m(\alpha(x))[Y_l^m(\alpha(y))]^* \tag{58}$$

where $r_<$ and $r_>$ are, respectively, the smallest and the largest of r. As shown in [18, Proposition 3.3], by interpreting $\frac{r_<^l}{r_>^{l+1}}$ as $-\frac{1}{2R^2}$, through an "averaging" procedure, the function μ in (56) can be recast as

$$\mu(\alpha(y)) = -2DT_\infty(y) + \int K_{\text{sph}}(\alpha(y),\, \alpha(x))\mu(\alpha(x))\, d\alpha(x), \tag{59}$$

where the integral kernel K_{sph} is given by

$$K_{\mathrm{sph}}(\alpha(x),\, \alpha(x)) = -\sum_{l=0}^{+\infty} \frac{1}{2l+1} \sum_{m=-l}^{m=l} Y_l^m(\alpha(y))[Y_l^m(\alpha(x)]^*.$$

Thus the solution μ in (59) may be written as

$$\mu(\alpha(x)) = -2D \int \left(I - K_{\mathrm{sph}}\right)^{-1} (\alpha(x),\, \alpha(y))\, T_\infty(\alpha(y))\, d\alpha(y),$$

where I denotes the unit operator, and the inverse of the linear operator $I - K_{\mathrm{sph}}$ is

$$\left(I - K_{\mathrm{sph}}\right)^{-1} (\alpha(x),\, \alpha(y)) = \sum_{l=0}^{+\infty} \frac{2l+1}{2l+2} \sum_{m=-l}^{m=l} Y_l^m(\alpha(x))[Y_l^m(\alpha(y))]^*.$$

Therefore,

$$-2D \int (I - K_{\mathrm{sph}})^{-1} (\alpha(x),\, \alpha(y))\, T_\infty(y)\, d\alpha(y) = \mu_{sph}(x) = \frac{|x|^2}{6} \tag{60}$$

which becomes on S_{sph} the expression $\mu(\alpha(y_S)) = \frac{R^2}{6}$. By reshuffling the above solution for $\mu_{\mathrm{sph}}(y)$ into equation (55), as shown in [18, Proposition 3.3], the MFPT function is

$$T(x) = T_{\mathrm{sph}}(x) = \frac{R^2 - |x|^2}{6D}, \tag{61}$$

which does satisfy the Dirichlet boundary condition (54) and agree with [14] and [18, Example 2.5].

Next, we turn to the MFPT function for a diffusing particle inside a sphere Ω of radius R with a Robin boundary condition on S_{sph}. Namely, the solution of the Poisson equation in the sphere with Robin boundary condition of type

$$D\Delta T(x) = -1 \text{ in } \Omega, \tag{62}$$

$$a \lim_{x \to y} \frac{\partial T}{\partial n}(x) + b \lim_{x \to y} T(x) + c = 0 \text{ on } S_{\mathrm{sph}}, \tag{63}$$

whenever $a \neq 0$, b and c being real constants, is given by

$$T_{Rob}(x) = T_\infty(x) + \int_{S_{\mathrm{sph}}} L_\infty(x,\, y,\, 0) \mu_{Rob}(y)\, dS(y), \tag{64}$$

where the density μ_{Rob} is defined by

$$\mu_{Rob}(y) = \frac{1}{a}\left(a\frac{\partial}{\partial n(y)} + b\right)\left(2DT_\infty(y) + 2D\int_{S_{\mathrm{sph}}} L_\infty(y, z, 0)\mu_{Rob}(z)\, dS(z)\right) + \frac{2Dc}{a}. \tag{65}$$

We introduce ${\mu_{Rob}}_l^m$ for μ_{Rob} (y on S_{sph}) in previous equation (65), using the counterpart of (23). Then, operating like for the above case of absorbing surface, equation (65) becomes

$${\mu_{Rob}}_l^m = \left(1 + \frac{2bR}{a}\right){\mu_{Rob}}_l^m + \int Y_l^m(\Omega_z)^*\left(\frac{1}{a}\left(a\frac{\partial}{\partial n(y)} + b\right)2DT_\infty(y) + \frac{2Dc}{a}\right).$$

One gets

$$\mu_{Rob}(\alpha(x)) = \int (I - K_{Rob})^{-1}(\alpha(x), \alpha(y))\left(\frac{1}{a}\left(a\frac{\partial}{\partial n(y)} + b\right)2DT_\infty(y) + \frac{2Dc}{a}\right)d\alpha(y), \tag{66}$$

$$(I - K_{Rob})^{-1}(\alpha(x), \alpha(y)) = \sum_{l=0}^{+\infty}\frac{2l+1}{2l - (2b/Ra)}\sum_{m=-l}^{m=l} Y_l^m(\alpha(x))[Y_l^m(\alpha(y))]^*.$$

One finds ${\mu_{Rob}}_l^m = 0$, for $l > 0$, and ${\mu_{Rob}}_0^0 = \sqrt{4\pi}\left(\frac{a}{3b} + \frac{R}{6} - \frac{cD}{bR}\right)$, so that

$$\mu_{Rob} = \frac{a}{3b} + \frac{R}{6} - \frac{cD}{bR} \tag{67}$$

and

$$T_{Rob}(x) = \frac{R^2 - |x|^2}{6D} + \frac{aR}{3bD} - \frac{c}{b}. \tag{68}$$

This T_{Rob} can be directly shown to agree with the solution of the Poisson equation (62) with Robin boundary condition (63). $(I - K_{Rob})^{-1}$, (67) and (68) display that $b \neq 0$ is necessary for the present reliability of the Robin boundary condition. In fact, the case $b = 0$ and $c = 0$ corresponds to the well-known non-existence of an MFPT solution inside an undeformed spherical surface with Neumann boundary condition.

Appendix B. Green's functions

We shall need the expansion of $L_\infty(x, y, 0)$ in cylindrical coordinates $x = (\rho, \varphi, z) = (x_2, z)$ and $y = (\rho', \varphi', z') = (y_2, z')$ given by

$$L_\infty(x, y, 0) = \frac{1}{4\pi D} \sum_{n=-\infty}^{+\infty} e^{i(\varphi-\varphi')} \int_0^{+\infty} e^{-\kappa|z-z'|} J_n(\kappa\rho) J_n(\kappa\rho')\, d\kappa, \tag{69}$$

where J_n is the standard regular Bessel functions of n-th order, see [29]. For general x,

$$2D \int_{S_c} L_\infty(x, \xi, 0) dS(\xi) = r \int_0^{+\infty} \left(2 - e^{-\kappa(h_1 - z)} - e^{-\kappa(z+h_1)}\right) \frac{J_0(\kappa\rho)}{\kappa} J_0(\kappa r) d\kappa, \tag{70}$$

$$2D \int_{S_c} \frac{\partial L_\infty(x, \xi, 0)}{\partial n(\xi)} dS(\xi) = r \int_0^{+\infty} \left(2 - e^{-\kappa(h_1 - z)} - e^{-\kappa(z+h_1)}\right) \frac{J_0(\kappa\rho)}{\kappa} \frac{dJ_0(\kappa\rho')}{d\rho'}\bigg|_{\rho'=r} d\kappa. \tag{71}$$

The integrands in (70) and (71) make the integral convergent for both small and large κ. (70) and (71), for different x, will play a crucial role in Section 4. The consistency of (70) and (71) will be confirmed by the following analysis and useful identities. The equation (69) yields

$$D\left(\Delta_2 + \frac{\partial^2}{\partial z^2}\right) \frac{\partial}{\partial \rho'} L_\infty((x_2, z), (y_2, z'), 0) = -\left(\frac{\partial}{\partial \rho'} \delta^{(2)}(x_2 - y_2)\right) \delta(z - z'), \tag{72}$$

where Δ_2 is the two-dimensional Laplacian with respect to x_2. On the other hand, let $G(x_2, y_2)$ be the two-dimensional Green's function. One has

$$G(x_2, y_2) = \frac{1}{2\pi} \sum_{n=-\infty}^{+\infty} e^{i(\varphi-\varphi')} g_n(\rho, \rho') \tag{73}$$

$$D\Delta_2 \frac{\partial}{\partial \rho'} G(x_2, y_2) = -\frac{\partial}{\partial \rho'} \delta^{(2)}(x_2 - y_2), \tag{74}$$

so that $g_0(\rho, \rho') = -D^{-1} \ln \rho_{max}$, and $g_n(\rho, \rho') = \frac{1}{2D|n|} (\rho_{min}/\rho_{max})^{|n|}$ for $n \neq 0$, where ρ_{min} and ρ_{max} are the smallest and the largest of ρ and ρ'. By applying the integral $\int_{-\infty}^{+\infty} dz$ to equation (72), noting that $\frac{\partial^2}{\partial z^2}$ yields a vanishing contribution and comparing with equation (74), one gets

$$\int_{-\infty}^{+\infty} \frac{\partial}{\partial \rho'} L_\infty((x_2, z), (y_2, z'), 0)\, dz = \frac{\partial}{\partial \rho'} G(x_2, y_2). \tag{75}$$

By comparing the right-hand-sides of equations (75) and (73), one gets, for $n = 0, 1, 2, \ldots,$

$$\frac{1}{D}\int_0^{+\infty}\frac{J_n(\kappa\rho)}{\kappa}\frac{\partial J_n(\kappa\rho')}{\partial\rho'}\,d\kappa=\frac{\partial g_n(\rho,\rho')}{\partial\rho'}. \tag{76}$$

For $n=0$, the integral in (76) is ambiguous when ρ' tends to $\rho=r$. The ambiguity is solved in [19, Example 1], yielding

$$\int_0^{+\infty}\frac{J_0(\kappa\rho)}{\kappa}\frac{\partial J_0(\kappa\rho')}{\partial\rho'}\,d\kappa=-\frac{1}{2r}. \tag{77}$$

which is crucial for the cancellation giving rise to (44). On the other hand, for $n\neq 0$ and ρ' tending to $\rho=r$, one gets from [19, Appendix C] that

$$\int_0^{+\infty}\frac{J_n(\kappa\rho)}{\kappa}\frac{\partial J_n(\kappa\rho')}{\partial\rho'}\,d\kappa=0. \tag{78}$$

Thus equation (76) provides a correction of a previous equation in [19, Appendix C] (relating $\int_{-\infty}^{+\infty}L_\infty dz$ to G). However, it turns out that such an equation in [19] also leads, in a formal sense, to equations (76), (77) and (78), thereby keeping the results in [19] valid.